Pyrogenic HONO seen from space: insights from global IASI observations.

https://doi.org/10.5194/egusphere-2023-2707

Response to Referee #2

In their manuscript, "Pyrogenic HONO seen from space: insights from global IASI observations," the authors present a new retrieval of HONO from biomass burning using the infrared sounder IASI. Franco et al. identify two absorption bands (820-890 cm-1 and 1210-1305 cm-1) for optimal use in the calculation of the hyperspectral range index (HRI), used in the detection of HONO. The authors demonstrate that the 1210-1305 cm-1 absorption band has the least interferences with ammonia (NH3) and dust in the Middle East. They reduce false detections of pyrogenic HONO by also using co-located NH3 and C2H4. Instead of focusing solely on individual fires as previous studies have done, the authors also present a global HONO detection climatology of fires from 2007 to 2023, analyzing HONO detection location, aerosol height, MODIS FRP count and mean FRP, and detection time of year. These parameters are compared against the TROPOMI UV-Vis HONO retrieval and a discussion about the differences in retrieval quality between the two instruments is provided. IASI is capable of outputting trace gas retrievals during the daytime and nighttime, and the authors use the number of IASI HONO detections and case studies to form hypotheses about the HONO diel cycle. Finally, Franco et al. use a neural network, ANNI, to compute HONO vertical column densities. These are qualitatively compared to TROPOMI.

This paper demonstrates a new and groundbreaking retrieval of pyrogenic HONO using infrared sensing that allows for long-term analysis of HONO and sub-diurnal observations without the aerosol sensitivity that the UV-Vis retrieval has. HONO has been shown to be critical in the early stages of fire plumes as it is the majority source of OH due to its short photolytic lifetime. How varying sunlight impacts HONO lifetime within smoke is a crucial topic of interest given its oxidative importance. This retrieval is also prime for use on new geostationary satellite (MTG-IRS) which will make observations has frequent as every half hour. This paper is thorough, well-structured, and written well. The limitations of each HONO retrieval method (IASI IR vs TROPOMI UV-Vis) are discussed and reiterated throughout the manuscript and was very appreciated by this reviewer. I recommend this paper for publication subject to minor revisions.

We thank the Referee for the positive evaluation of the paper and for the constructive comments that helped improving the manuscript. Please find in blue here below our answers to the Referee's comments and the changes made to the manuscript. Additionally, we have updated some figures to enhance their clarity. Furthermore, we have revised several figures to improve both their clarity and consistency across the entire manuscript.

General Comments:

I thought the authors did a great job presenting their work, arguments, and conclusions to the reader. The following are a few general comments:

The authors ultimately decided to show many of their results using the 1210-1305 cm-1 window due to the limitations shown for the 820-890 cm-1 window (NH3 interference and Middle East dust interference) and I was curious why this window was included for earlier discussion in the paper. The

conditions defined in lines 252-253 made me wonder why this is defined since it has a demonstrated surface emissivity anomaly and NH3 interference. Line 285 also mentions using the two different HONO HRIs right after the authors state that only the 1210-1305 cm-1 window would be used from then on. It would make for a cleaner story if the 820-890 cm-1 window was not included at all and just summarized as a window that was up for consideration.

We thank the Referee for this comment. Throughout Sect. 2, we systematically examined both the 820-890 and 1210-1305 cm^{-1} spectral ranges for HONO detection. We firmly believe that, especially at this stage of the manuscript, it is crucial to give equal consideration to both bands. Notably, the 820-890 cm^{-1} absorption feature led to the first identification and retrieval of HONO with infrared satellite sounders (Clarisse et al., 2011; Dufour et al., 2022). Therefore, in Sect. 2, we conducted various exercises to evaluate both bands, including a comparison of HRI intensity in fresh fire plumes (Sect. 2.2), a thorough spectral analysis with the whitening (Sect. 2.3), and a comparison of the specific detection filters set up for each absorption band (Sect. 2.4). While we concluded Sect. 2.4 by specifying our focus on the 1210-1305 cm^{-1} HRI for the rest of the study, we deliberately included some results from the 820-890 cm^{-1} range in our analysis in Sect. 3 (and related figures in appendix) as it allows us to perform comparisons between the two HONO bands. The consistency observed in our results across these two ranges provides indeed valuable cross-verification, bolstering the robustness of our findings. We are convinced that this approach is important for establishing the reliability of our methodology and results, and that it enhances the overall strength and credibility of our study.

To clarify our approach, we have added the following statements, respectively, in Sect. 2.1 and at the end of Sect. 2.4:

Line 132: "*Throughout Sect. 2, we systematically assess the advantages and limitations of each spectral range for the detection of pyrogenic HONO.*"

Line 278: "*Considering the advantages presented in Sect. 2 of the 1210-1305 cm^{-1} band for the detection of pyrogenic HONO by IASI, we will focus on the HRI calculated within this range from Sect. 3 onwards. Nonetheless, results obtained with the 820-890 cm^{-1} band will also be presented briefly, as they allow for important cross-verification.*"

Many of the figures referenced in the paper do not have the subpanels added to direct the reader to the specific panel the authors are referring to. For example, line 192 talks about the retrieved spectrum, which is in Figure 2a, line 203 talks about NH3 interferences, which is in Figure 2b, line 258 talks about non simultaneous detection of NH3 and C2H4, which can be easily seen in Figures 3c, d, and h, etc. These cues make it easier for the reader to follow the authors' line of thought.

We thank the Referee for this suggestion, which contributes to enhancing the paper's clarity. In the revised manuscript, we have increased the frequency of references to figures, specifically pinpointing relevant panels crucial to the ongoing discussion.

Specific Comments:

Figure 1: I suggest adding wind vectors over each panel to demonstrate where the HONO is being transported from. I think it would be especially helpful in Figures 1c and 1d, the October 15, 2017 9:30 PM overpass. Additionally, it would aid the reader if a general HRI = 4 contour was included in each subfigure. Finally, I suggest making the red cross either a square or a thick outline. My initial thought was that a red cross meant bad data, ignore this.

We thank the Referee for these suggestions. Please find below the revised version of Fig. 1.

- Panels c and d incorporate the wind vectors associated with each IASI/Metop-A observation, derived from the daily horizontal wind fields from the ECMWF ERA5 reanalysis (Hersbach et al., 2020). The wind is oriented to the North and carries the fire plume above the Bay of Biscay.
- Unfortunately, adding an HRI = 4 contour line was not feasible due to significant variations in HONO HRI among nearby IASI observations and the discontinued spatial sampling. However, to enhance differentiation between HRI>4 and HRI<4 observations, we have modified the colour palette, which is now discretized, and IASI observations with HRI<4 are displayed with semi-transparency.
- We have replaced the red cross by a light blue square around the observation of interest.

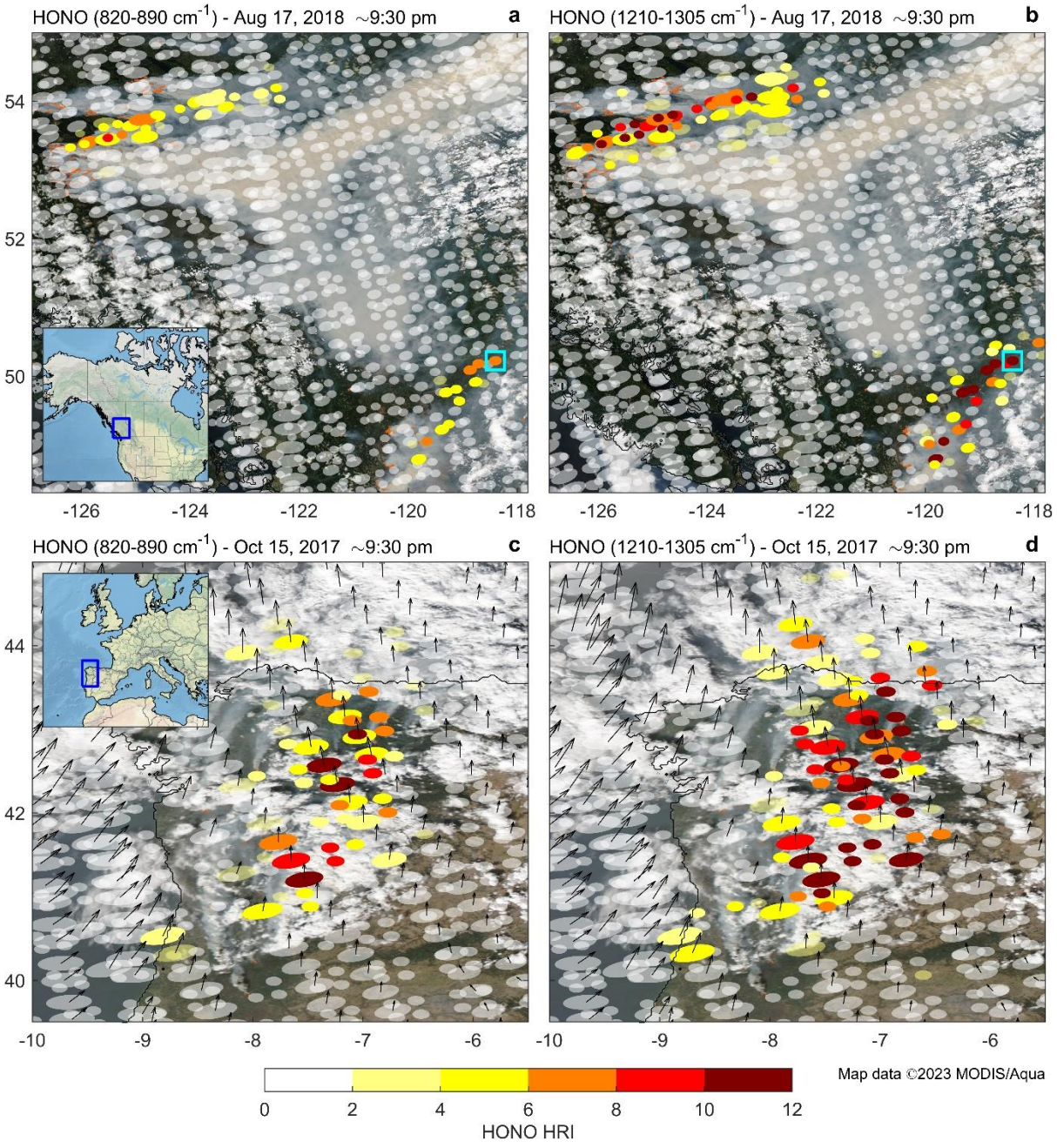

Line 195: Could the authors include an appendix figure covering the entire spectral interval? It makes me curious why 1210-1250 cm-1 was omitted.

The figure below displays Fig. 2, including the entire 1210-1305 cm^{-1} spectral range in panel c and the whitened NH_3 Jacobian. The 1210-1250 cm^{-1} range shows no significant contribution of HONO to the HRI, and there is no interference from NH_3, as NH_3 lacks absorption features in that part of the spectrum. We intentionally selected a wide range (1210-1305 cm^{-1}) for calculating the HONO HRI to provide more baseline, reducing issues related to, for example, surface emissivity. However, for better visibility of the HONO absorption features around 1264 cm^{-1}, we prefer to zoom in on the 1250-1305 cm^{-1} range in Fig. 2.

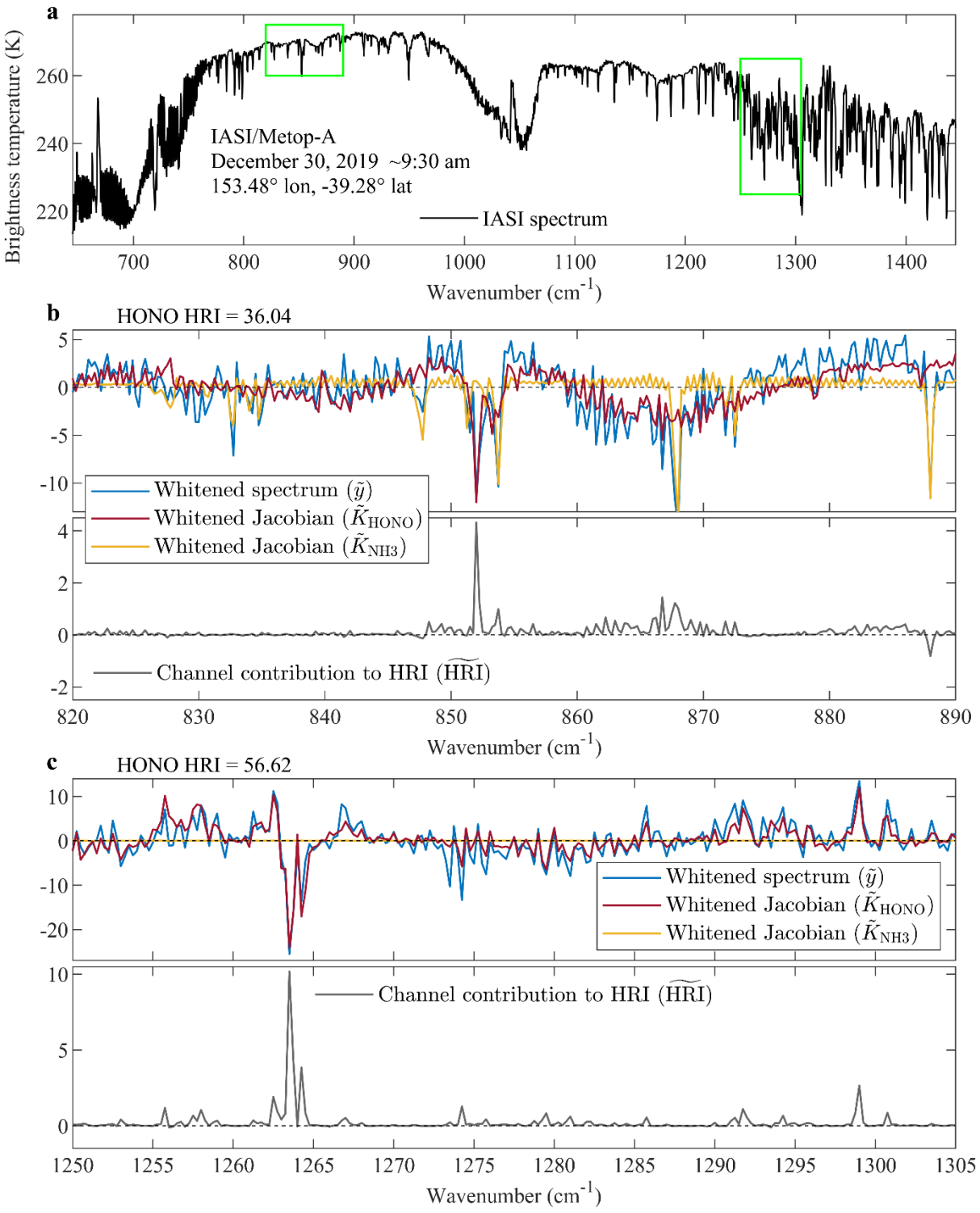

Section 2.3: I was confused what the author meant by the term “channel,” as in the channel contribution to HRI. I first thought it was for each individual compound, but then Figure 2b talks about the channel contribution to HRI for both HONO and NH3 referencing the same line. It may have been defined in a referenced paper or it may be common terminology in this specific field. However, I would like more context or a clear definition.

A “channel” is defined here as the observed IASI radiance at a specific wavenumber. It corresponds to a single spectral band sampled at 0.25 cm^{-1}, which is the spectral resolution of IASI (after apodization). We have added this definition to the manuscript.

Figure 2: Could the whitened Jacobian for NH3 also be added to c? Would this further demonstrate a lack of interference from NH3?

We appreciate the suggestion from the Referee. We have now included the whitened NH_3 Jacobian in panel c of Fig. 2 (and in the other similar figures in the appendix). As mentioned earlier, NH_3 lacks absorption features in that part of the spectrum and, therefore, cannot influence the HONO HRI in that band.

Line 232: Can these localized surface emissivity anomalies be accounted for in the retrieval or are they time-varying properties?

A first-order correction could be applied by estimating the spatially variable biases from a period in the year (usually the winter), as done by Clarisse et al. (2019) for the retrieval of dust from IASI. The prerequisite of such approach is to assume that the emissivity and corresponding bias is constant throughout the year (or at the least has less variability than the bias itself). However, the surface emissivity anomalies affecting the 820-890 cm^{-1} HONO absorptions are spatially too heterogeneous, too intense, and too time-of-the-year-dependent to be efficiently accounted for.

Figure 3: Is there any reason why it looks like there are more than two populations in the HONO vs NH3 colored by C2H4 figures (Figures 3a, c, e, and g)? It is especially apparent in 3a, where a linear trend of yellow dots seems distinct from the pink/orange dots of higher NH3, but lower HONO. Could the authors discuss this? It may be relevant to the biomass type and region comment in lines 257-258.

The population highlighted by the Referee in Fig. 3a (for the 820-890 cm^{-1} range), also noticeable in Fig. 3e (for the 1210-1305 cm^{-1} range), is mainly associated with the 2009 and 2019/2020 Australian wildfires. This population is less evident in the scatter plots including the pm observations (Figs 3c and g), given that the number of HONO detections is roughly 10 times higher in nighttime than in daytime. What is notable about these specific events is that they resulted in numerous HONO detections during both daytime and nighttime overpasses, with particularly high C_2H_4 HRI values but not very high NH_3 HRI values compared to other fire events. Various factors, such as the type of vegetation burned, high loads of smoke aerosols (which are hypothesized to shield the HONO burden from efficient photolysis, extending its lifetime), and intense pyroconvection transporting fire plumes to the lower stratosphere where photochemistry is slowed drastically (increasing competition for OH), are among many elements that can explain the specificity of Australian fire plumes. Although we agree with the Referee that delving further into the population of points in Fig. 3 is undoubtedly interesting, we believe it is not possible to do so within the framework of this paper and that it would deserve a dedicated study.

Line 289-290: Is there any other data that would explain these random detections over remote ocean?

The HONO detection filter we set up effectively mitigates random detections over remote oceans. Nevertheless, given the extensive IASI time series, it is conceivable that a limited number of observations might bypass the filter, though such instances remain largely marginal, as evident in Figs 4 and A5. These random detections constitute only ~20 instances out of the >10 x 10^9 observations in the entire IASI time series. We identify ice clouds, characterized by broadband infrared observations, as a potential interference leading to these random detections. For instance, in Fig. 4, two of these random detections are visible over Antarctica.

Line 316: The authors later go into an analysis of why there are detections lacking in the global tropics (sect 3.2), but I was curious what is the effect of clouds on the retrievals? I know that the authors included cloud and cloud-free spectra, but there wasn't a comment on how clouds affect the retrieval. I asked myself if the ITCZ had any effect? This may be showing my lack of IR expertise.

The HRI has indeed been built based on a subset including cloudy and cloud-free spectra, ensuring that the HRI remains unbiased for all atmospheric conditions. However, if the cloud coverage is too thick and extensive, the detection of HONO will be impeded (the HRI values will be very weak), and the IASI measurements will simply not pass the HONO detection filter, and no retrieval will be performed. This implies that the retrieval of HONO is primarily conducted for cloud-free scenes and for observations with a limited cloud cover. Such residual clouds typically impact the baseline of the spectra. However, since we use surface temperature instead of a baseline temperature derived from the spectrum, the residual clouds have only a marginal impact on the HONO detection and retrieval. Additionally, in the final product, we provide a cloud flag that allows the user to discriminate between clear-sky, partially cloudy, and cloudy scenes.

We do not believe that the ITCZ plays a role in the small number of HONO detection within the Tropics. For instance, during the Northern Hemisphere winter (Nov – Feb), the ITCZ moves southward, leading to dry and hot weather in western and central Africa. This corresponds to the biomass burning season, as shown in Fig. 5. Even though the ITCZ is located to the south during this period, IASI does not detect HONO during the fire season of these regions.

Figure 5: I found it interesting that IASI HONO saw detections off the coast of Australia, over water. How does this retrieval do over water? There was a large discussion of the thermal contrast affecting the retrieval. Were these plumes detected because they were over water or because the strength of the fires had lofted them high enough for key detection?

The ANNI v4 retrieval performs equally well over both land and sea. The crucial factor lies in the ability to detect HONO, which is largely dependent on thermal contrast. Typically, thermal contrast is weaker over water than over land. However, the Australian wildfires are well known for their intense pyroconvection that swiftly lifted concentrated PyroCb to the UTLS, reaching altitudes of 14-16 km off the coast of Australia. The air temperature at such altitudes is very low, resulting in a very large thermal contrast with the surface. Both the large thermal contrast and the high concentrations in trace gases favoured the detection of HONO over water during these fire events.

Equation 6: I'm not sure why this equation is presented, if only to demonstrate height dependence on the detection threshold. When the authors talk about the NN VCD calculation in section 4, I was wondering if this equation was used or not.

Eq. 6 is used in Sect. 3.2 to characterize the HONO VCD that corresponds to the IASI generalized noise, and hence to the detection threshold, for a standard atmosphere, depending on the plume altitude. However, as explained in Sect. 4.1, the actual retrieval of the HONO VCD for a single IASI observation is performed using an artificial NN. This NN is provided with the single pixel HRI – and ancillary variables describing the state of the surface and atmosphere – and yields an estimate of the HONO VCD. Eq. 6 does not play a role in this process.

Line 376: This line made me wonder what the height limitations are on HONO detection with IASI.

The detection of HONO with IASI is particularly challenging in the lowermost atmospheric layers, especially in the planetary boundary layer, owing to the overall weak thermal contrast between the surface and these layers. As illustrated in Fig. 7, detecting HONO in these low layers with IASI

necessitates a substantial abundance of HONO, typically exceeding 2.5-3 x 10^{16} molec cm^{-2}, a condition that is rarely met.

Line 377: The authors spend a lot of time explaining their constraints for IASI HONO detection, but not a lot of time is spent explaining the constraints on valid TROPOMI HONO detections, which are frequently compared against.

While the scope of this study is HONO measurements with IASI, the manuscript also addresses constraints affecting HONO detections and retrieval with TROPOMI. For instance:

- The presence of smoke aerosols hindering TROPOMI from probing through the full height of the smoke plume is discussed in Sect 4.4.
- The difficulty in estimating the AMF to convert TROPOMI's SCDs to VCDs is also discussed in Sect. 4.4. Moreover, for a comprehensive description of TROPOMI's detection and retrieval, including limitations, readers are referred to Theys et al. (2020).
- As noted in the introduction, UV-Vis instruments like TROPOMI do not provide measurements during nighttime, when HONO's lifetime is expected to be the longest. Moreover, the manuscript discusses the impact of TROPOMI's overpass time (~1:30 pm), which coincides with the time of the day when HONO photolysis is most efficient.
- In Sect. 3.2, there is a discussion about the typical TROPOMI's detection threshold for HONO, which is significantly lower than IASI, and relatively homogeneous throughout the troposphere since, unlike IASI, TROPOMI's measurements are not influenced by the thermal contrast.

Line 390: Why is volcanic ash included?

While we do not anticipate any HONO detections associated with volcanic plumes, we have observed several instances in the CALIPSO data where "elevated smoke" was mistakenly classified as "volcanic ash", and vice versa.

Line 395: Did your analysis lead to the conclusion that layers between 2 and 4 km contained many false detections? I'd like to see this in an appendix figure or have a paper cited.

We realize that our statement in Lines 396-397 was misleading. What we meant to convey is that the low-altitude layers between 2 and 4 km can be influenced by anthropogenic pollution plumes exiting the planetary boundary layer, while in this study, we primarily measure HONO in mid- and high-altitude plumes. We have corrected our sentence: "*[…] numerous low-altitude layers comprised typically between 2 and 4 km, which may be influenced by anthropogenic pollution plumes.*"

Figure 8: Please add latitude labels.

We tried adding labels but found these too distracting. We clarified them instead in the caption: "*Parallels are drawn every 15° and meridians every 30°.*" For consistency, we did the same for the other figures using the same type of projection in the manuscript (Figs 5, 6, 8, and 12).

Figure 9: Are the MODIS fire detections in comparison to TROPOMI from Aqua or Terra, or both? Should TROPOMI be compared to the closest overpass? Or what about in comparison to VIIRS which has a very close overpass time to TROPOMI?

We thank the Referee for this question. So far, we have compared both IASI and TROPOMI to MODIS/Terra in Fig. 9. We agree that it is indeed more appropriate to compare TROPOMI with MODIS/Aqua, which has a coincident overpass time with TROPOMI (~1:30 pm). Please find the revised version of Fig. 9 below. Considering the similarities between the MODIS/Terra and MODIS/Aqua

distributions, note that the entire discussion and the conclusions related to this figure in the manuscript remain entirely valid.

Since MODIS/Aqua has a coincident overpass time with TROPOMI, we prefer to work only with MODIS for consistency throughout the manuscript and to avoid introducing an additional satellite dataset in the study.

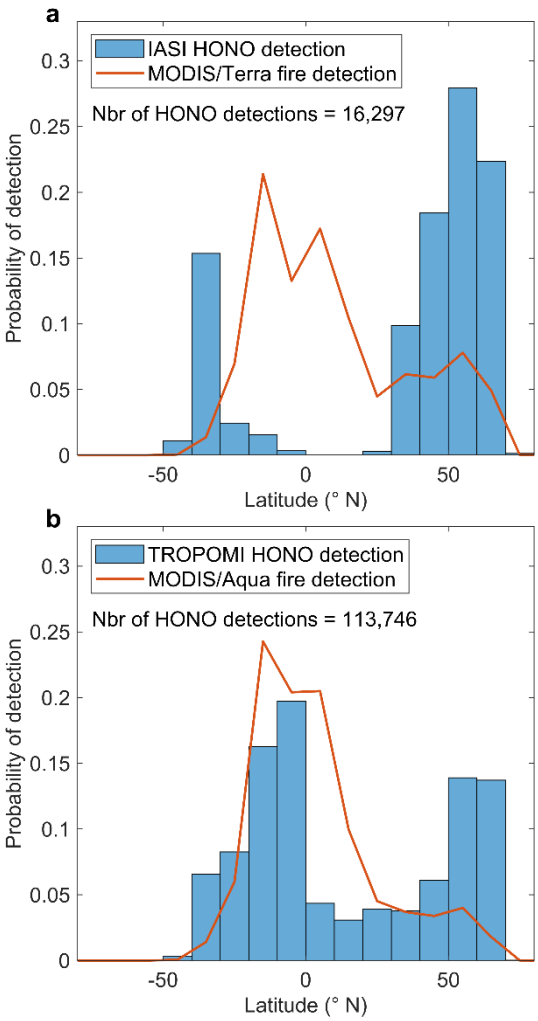

Figure 10: I may have missed it, but is there a reference comparing the differences between IASI-A, -B, and -C? I am seeing slight differences between the three instruments, though the authors show similar annual counts of HONO detections in Figure 11.

Overall, the three IASI instruments demonstrate excellent agreement during their overlapping years (Bouillon et al., 2020). The slight differences seen between IASI-A, -B, and -C in Fig. 10 are due to small variations in overpass times (~30 min) and spatial shifts between the tracks of the three Metop satellites. For instance, despite the 2200 km swath covered by a single IASI instrument, gaps exist in the Tropics between the successive orbits of this instrument. The tracks of the other instruments are set up to cover the tropical gaps left by the first instrument. Consequently, a specific fire plume is never sampled simultaneously, and with the same spatial coverage, by each IASI instrument, leading to different numbers of HONO detections for these instruments in the same fire plume.

When aggregated over all the fire events detected throughout the course of one year of observation, these differences largely cancel out, contributing to the consistency observed between the three IASI instruments in Fig. 11.

Line 440: What is a confirmed HONO detection?

We consider HONO detections as “confirmed” those that passed the specific filter set up in Sect. 2.4. To avoid creating ambiguities, we have changed "*the number of confirmed HONO detections*" to "*the number of HONO detections*" in this sentence.

Line 452: Has anyone else cited this drop in the year 2022? Not for HONO detections but perhaps in sum FRP? Very interesting.

While we are not aware of recent studies reporting a drop in 2022, considering the devastating biomass burning season in North America in 2023, more studies on the topic will likely emerge. Nonetheless, the Referee’s question has motivated us to investigate this point further. In the revised version of Fig. 11 (below), we have presented the annual cumulative Fire Radiative Power (FRP) from MODIS/Terra for the Northern Hemisphere mid and high latitudes (>30° N) from 2007 to 2022 (the consolidated MODIS dataset is not available yet for the entire 2023). This cumulative FRP is the sum of all individual fire contributions throughout each year, providing a better indicator of integrated biomass combustion than, for example, fire count (which disregards fire magnitude) or average FRP (which ignores the number of fires). For consistency, we now consider only the HONO detections above 30° N since those represent by far most of the detections. In this figure, we observe that the cumulative FRP closely follows the time series of HONO detections, with drops in 2016 and 2022 and a peak in 2021, aligning with the IASI data. This represents additional evidence indicating that HONO detection with IASI depends strongly on fire intensity. We have included this revised figure in the manuscript, and we now discuss this in Sect. 3.3.

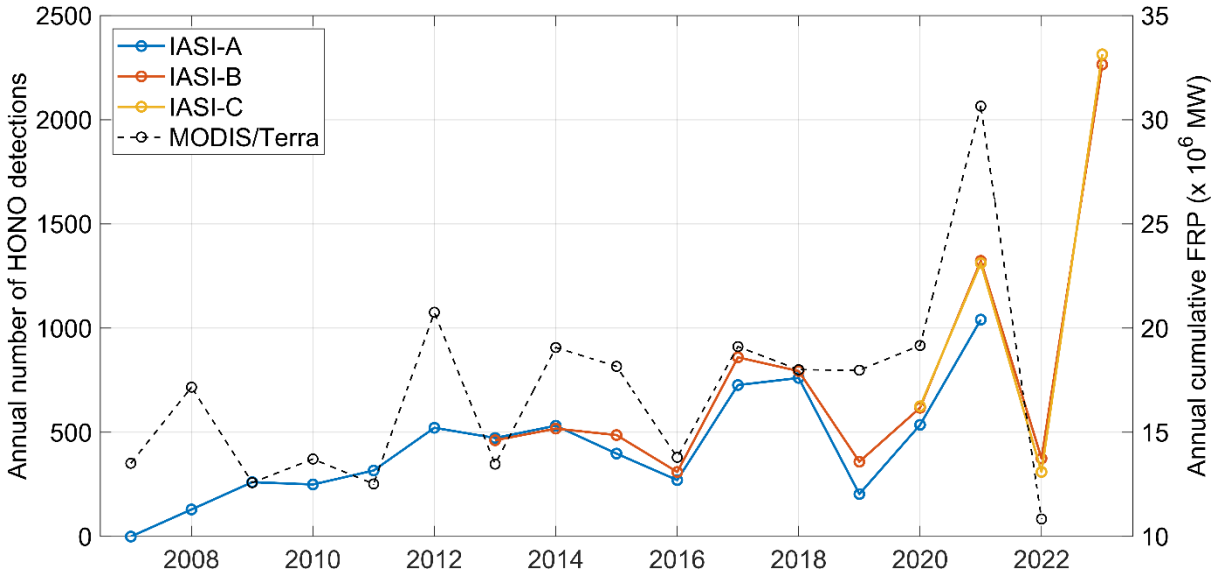

Section 3.4: One paragraph starts by saying “To rule out potential other reasons for the observed am/pm difference…” but then the section doesn’t have an overall concluding statement about HONO’s diel cycle, just about the effect of photochemistry on C2H4

We thank the referee for highlighting this point. We have included the following concluding statement in the C_2H_4 analysis:

“To rule out potential other reasons for the observed am/pm difference, it is useful to look at another short-lived biomass burning tracer, namely C_2H_4. In Fig. 12, we compare […]

[…] Although reactions with OH and O_3 are expected to proceed more slowly during nighttime hours due to lower temperatures, we do not observe a prevalence of C_2H_4 detections with the evening IASI measurements, such as observed for HONO (Fig. 12). This suggests, first, that variations in photochemistry between daytime and nighttime do not significantly impact C_2H_4 concentrations in fire plumes. Second, it implies that the presence of measurement artefacts responsible for large am/pm differences in HONO detection can be ruled out, confirming that the absence of photolysis is the primary driver of the more numerous HONO detections at nighttime."

Technical Corrections:

Line 377: "An HONO detection" to "A HONO detection."

Corrected

References

- Clarisse, L., R'Honi, Y., Coheur, P.-F., Hurtmans, D., and Clerbaux, C.: Thermal infrared nadir observations of 24 atmospheric gases, Geophysical Research Letters, 38, L10802, https://doi.org/10.1029/2011gl047271, 2011.
- Dufour, G., Eremenko, M., Siour, G., Sellitto, P., Cuesta, J., Perrin, A., and Beekmann, M.: 24 h Evolution of an Exceptional HONO Plume Emitted by the Record-Breaking 2019/2020 Australian Wildfire Tracked from Space, Atmosphere, 13, 1485, https://doi.org/10.3390/atmos13091485, 2022.
- Hersbach, H., Bell, B., Berrisford, P., Hirahara, S., Horányi, A., Munoz-Sabater, J., Nicolas, J., Peubey, C., Radu, R., Schepers, D., Simmons, A., Soci, C., Abdalla, S., Abellan, X., Balsamo, G., Bechtold, P., Biavati, G., Bidlot, J., Bonavita, M., Chiara, G., Dahlgren, P., Dee, D., Diamantakis, M., Dragani, R., Flemming, J., Forbes, R., Fuentes, M., Geer, A., Haimberger, L., Healy, S., Hogan, R. J., Hólm, E., Janisková, M., Keeley, S., Laloyaux, P., Lopez, P., Lupu, C., Radnoti, G., Rosnay, P., Rozum, I., Vamborg, F., Villaume, S., and Thépaut, J.-N.: The ERA5 global reanalysis, Quarterly Journal of the Royal Meteorological Society, 146, 1999–2049, https://doi.org/10.1002/qj.3803, 2020.
- Walker, J. C., Dudhia, A., and Carboni, E.: An effective method for the detection of trace species demonstrated using the MetOp Infrared Atmospheric Sounding Interferometer, Atmospheric Measurement Techniques, 4, 1567–1580, https://doi.org/10.5194/amt-4-1567-2011, 2011.